HHS Public Access

Author manuscript

Hum Brain Mapp. Author manuscript; available in PMC 2020 February 01.

Published in final edited form as:

Hum Brain Mapp. 2019 February 01; 40(2): 566–577. doi:10.1002/hbm.24395.

From Eyes-closed to Eyes-open: Role of Cholinergic Projections in EC-to-EO Alpha Reactivity Revealed by Combining EEG and MRI

Lu Wan[1,†], **Haiqing Huang**[1,2,†], **Nadine Schwab**[3], **Jared Tanner**[3], **Abhijit Rajan**[1], **Ngoc B. Lam**[1], **Laszlo Zaborszky**[4], **Chiang-shan R. Li**[5], **Catherine C. Price**[3], and **Mingzhou Ding**[1,*]

[1.]J. Crayton Pruitt Family Department of Biomedical Engineering, University of Florida, Gainesville, FL 32611.

[2.]Department of Psychology, University of Pittsburgh, Pittsburgh, PA 15260

[3.]Department of Clinical & Health Psychology, University of Florida, Gainesville, FL 32611

[4.]Center for Molecular and Behavioral Neuroscience, Rutgers University, Newark, NJ 07102

[5.]Departments of Psychiatry and Neuroscience, Yale University School of Medicine, New Haven, CT 06510

Abstract

Alpha rhythm (8 to 12 Hz) observed in EEG over human posterior cortex is prominent during eyes-closed (EC) resting and attenuates during eyes-open (EO) resting. Research shows the degree of EC-to-EO alpha blocking or alpha desynchronization, termed alpha reactivity here, is a neural marker of cognitive health. We tested the role of acetylcholine in EC-to-EO alpha reactivity by applying a multimodal neuroimaging approach to a cohort of young adults and a cohort of older adults. In the young cohort, simultaneous EEG-fMRI was recorded from twenty-one young adults during both EO and EC resting. In the older cohort, functional MRI was recorded from forty older adults during EO and EC resting, along with FLAIR and diffusion MRI. For a subset of twenty older adults, EEG was recorded during EO and EC resting in a separate session. In both young and older adults, functional connectivity between the basal nucleus of Meynert (BNM), the major source of cortical acetylcholine, and the visual cortex increased from EC to EO, and this connectivity increase was positively associated with alpha reactivity; namely, the stronger the BNM-visual cortex functional connectivity increase from EC to EO, the larger the EC-to-EO alpha desynchronization. In older adults, lesions of the fiber tracts linking BNM and visual cortex quantified by leukoaraiosis volume, associated with reduced alpha reactivity. These findings support a role of acetylcholine and particularly cholinergic pathways in mediating EC-to-EO alpha reactivity and suggest that impaired alpha reactivity could serve as a marker of the integrity of the cholinergic system.

[*]**Corresponding Author:** Mingzhou Ding, Phone: +1-352-273-9332, Fax: +1-352-273-9221, MDing@bme.ufl.edu.
[†]Lu Wan and Haiqing Huang should be considered joint first author.

Keywords

Alpha reactivity; acetylcholine; basal nucleus of Meynert; leukoaraiosis; eyes-closed; eyes-open; resting state

1. INTRODUCTION

For over 80 years we have known that the magnitude (power) of occipital alpha oscillations reduces from the eyes-closed (EC) resting to eyes-open (EO) resting (Adrian & Matthews, 1934; Berger, 1933; Jasper, 1936; Smith, 1938). Such alpha blocking or desynchronization is often taken as an indicator of visual cortex activation (Chapman et al., 1962; Gale et al., 1971; Glass & Kwiatkowski, 1970; Hardle et al., 1984; Legewie et al., 1969; Volavka et al., 1967); the underlying neural mechanisms remain unclear. Recent studies further suggest that alpha reactivity from EO to EC may associate with cognitive health especially in the aged population (Babiloni et al., 2010; Duffy et al., 1984; Hanslmayr et al., 2005). In fact, in older adults, it has been shown that reduced alpha reactivity may serve as a possible marker for the onset of Alzheimer's disease (McBride et al., 2014). Thus, understanding the neural substrate of alpha reactivity has both basic and clinical neuroscience significance.

As a neurotransmitter that plays a significant role in cortical activation and arousal, researchers have extensively studied the anatomy and function of acetylcholine (ACh) in animal models (Detari & Vanderwolf, 1987; Metherate et al., 1992). Human EEG work has further found that ACh modulates alpha activity (Feige et al., 2005). To what extent ACh contributes to EC-to-EO alpha reactivity has not been systematically investigated. Past research on ACh in humans has mainly relied on observing the effects of cholinergic drugs (Bauer et al., 2012; Meador et al., 1989; Silver et al., 2008). However, the effects of cholinergic drugs are systemic, not limited to the brain, and their administration can have adverse effects, especially in older individuals (Mintzer & Burns, 2000; Rudolph et al., 2008).

Recent neuroimaging studies have made an alternative nonperturbative approach viable by providing a stereotaxic probabilistic map of the basal nucleus of Meynert (Zaborszky et al., 2008). Anatomically, the basal nucleus of Meynert (BNM), lying anterior to the thalamus and basal ganglia, contains the cell bodies of neurons that provide cholinergic innervation of the cerebral cortex (Mufson et al., 2003; Raghanti et al., 2011; Whitehouse et al., 1982; Zaborszky et al., 2015; Zaborszky et al., 2012). Neuronal activities in BNM have been associated with memory formation (Richardson & DeLong, 1988), attention (Muir et al., 1993; Voytko et al., 1994), and the regulation of arousal and sleep (Thiele, 2009; Wenk, 1997). A recent empirical study indicated that BNM activation is significant for improving sensory processing by increasing reliability and decreasing redundancy in the cortex and thalamus (Goard & Dan, 2009). In this study, we used the functional connectivity between BNM and cortex, in lieu of cholinergic drugs, to test the role of ACh and associated cholinergic pathways in alpha reactivity in young and older adults.

Cholinergic axons linking BNM and cortex are mostly unmyelinated (Selden et al., 1998) and thus more vulnerable to aging-related vascular changes in the brain. These fibers pass

through areas near the anterior corpus callosum and the frontal horns of the ventricles where pathological changes of white matter, known as leukoaraiosis or LA, are common, particularly among older adults (Hachinski et al., 1987; Pantoni & Garcia, 1997). Specifically, LA occurs in 15 to 65% of adults (Breteler et al., 1994; Schmidt et al., 1999; Ylikoski et al., 1993), with a three-fold increase in older relative to younger adults (Hogervorst et al., 2002), and has been associated with such age-related disorders as Alzheimer's disease and small vessel dementia (Price et al., 2012; Price et al., 2015). We used LA along the cholinergic axons as naturally occurring lesions to further test the role of BNM and ACh projections in modulating EC-to-EO alpha reactivity.

Two cohorts of participants were recruited for this study. In both the cohort of young adults and the cohort of older cognitively well adults, EEG and fMRI data were acquired during eyes-closed and eyes-open resting state. Diffusion MRI and FLAIR MRI were further acquired from the older participants to assess fiber integrity and the extent of LA load. We investigated the neural substrate of alpha reactivity by (1) examining how BNM-cortex functional connectivity is related to alpha reactivity and (2) assessing the effects of LA severity within the cholinergic fiber system on alpha reactivity.

2. MATERIALS AND METHODS

Two datasets were acquired and analyzed here: one from young adults and the other from older adults. They were henceforth referred to as the "Young Dataset" and the "Old Dataset" respectively. Below we describe each dataset in detail.

2.1. Participants and Experimental Design

2.1.1. Young Dataset—The experimental protocol and data acquisition procedure were approved by the Institutional Review Board of the University of Florida (UF IRB). Twenty-one healthy college students (7 females; mean age: 20.5±2.93) with normal or corrected-to-normal vision gave written informed consent and participated in the study in exchange for course credit.

The experiment consisted of two resting-state simultaneous EEG-fMRI sessions each lasting 7 minutes. During one session, participants were instructed to remain still, stay awake, not to think any systematic thoughts, and keep eyes closed. During the other session, they were told to keep eyes open and fixate the cross at the center of an MR-compatible monitor, with other instructions remaining the same. The order of the two sessions was randomized across participants (Mo et al., 2013).

2.1.2. Old Dataset—Participants were recruited from a separate federally-funded and UF IRB-approved investigation involving non-demented cognitively well individuals and a prospective neuroimaging protocol involving structural and functional imaging sequences. The inclusion/exclusion criteria were: 1) aged 60 or older, 2) English as the primary language, 3) have intact activities of daily living, and 4) have baseline neuropsychological testing unsupportive for dementia criteria per Diagnostic and Statistical Manual of Mental Disorders – Fifth Edition (Association, 2000). All had to have a Telephone Screening for Cognitive Status (TICS) score greater than 30 (Barber & Stott, 2004). Additional exclusion

criteria included: a history of head trauma/ neurodegenerative illness, documented learning or seizure disorder, less than a sixth grade education, substance abuse in the last year, major cardiac disease, chronic medical illness known to induce encephalopathy, implantable device precluding an MRI, and an unwillingness to complete the MRI. Two neuropsychologists reviewed cognitive data and confirmed that test scores met the expected ranges for non-demented individuals.

Forty participants signed the written informed consent form and participated in the study. See Table I for their demographic information. All forty participants underwent structural, diffusion and functional MRI. A subset of twenty individuals completed additional scalp EEG recording with EC and EO conditions. One participant was excluded due to later identification of a lacune in the caudate nucleus. Demographic information for the final 19 participants can be found in Table II.

The experiment consisted of separate MRI and EEG recording sessions. Eyes-closed functional MRI were recorded for 7.5 minutes, during which participants were instructed to remain still, stay awake, and avoid any systematic thoughts. From two runs of n-back task-fMRI, we were able to extract 2-min of eyes-open resting state fMRI, according to previously published procedures (Fair et al., 2007). In a separate EEG recording session, the participants underwent 2 sessions of 2-min eyes-closed and 2 sessions of 2-min eyes-open resting states; the order of EC and EO sessions were randomized across participants.

2.2. Data Acquisition

2.2.1 Young Dataset

MRI acquisition.: Functional images were acquired on a 3-Tesla Philips Achieva whole-body MRI system (Philips Medical Systems, Netherlands) using a T2*-weighted echoplanar imaging (EPI) sequence (echo time (TE) = 30ms; repetition time (TR) =1980 ms; flip angle=80°). Two hundred and twelve (212) volumes of functional images were acquired during each resting-state session (EC and EO), with each whole-brain volume consisting of 36 axial slices (field of view: 224mm; matrix size: 64×64; slice thickness: 3.50 mm; voxel size: 3.5×3.5×3.5mm). A T1-weighted high resolution structural image was obtained for each participant after the two resting-state sessions (Mo et al., 2013).

EEG acquisition.: EEG data were recorded simultaneously with fMRI using a 32-channel MR-compatible EEG system (Brain Products GmbH, Germany). Thirty-one sintered Ag/AgCl electrodes were placed according to the 10–20 system and one additional electrode was placed on the participant's upper back to monitor electrocardiogram (ECG). ECG was used subsequently to aid the removal of the cardioballistic artifact. The impedance from all scalp channels was kept below 10 kΩ during the entire recording session as recommended by the manufacturer. The online band-pass filter had cutoff frequencies at 0.1 and 250 Hz. The filtered EEG signal was then sampled at 5 kHz, digitized to 16 bit, and transferred to the recording computer via a fiber-optic cable. The EEG recording system was synchronized with the scanner's internal clock throughout the recording session. The synchronization, together with the high sampling rate, was essential to ensure successful removal of the gradient artifact (Mo et al., 2013).

2.2.2 Old Dataset

MRI acquisition.: Functional MRI, diffusion MRI, isovoxel 3D T1 images, and T2 FLAIR images were acquired from all 40 participants on a Siemens MAGNETOM Verio 3T whole-body MRI scanner with an 8-channel head coil. For eyes-closed resting state scan, 7.5 minutes of fMRI were recorded using a single-shot EPI sequence with the following parameters: field of view=224mm×224mm, matrix size=64×64, TR=2s, TE=30ms, flip angle=90º, slice thickness=3.5 mm, 225 scans, and each volume consisting of 36 axial slices. Two runs of 7.5 minutes task-fMRI were recorded using the same sequence during which participants performed an n-back working memory task (see Figure S2 of the supplementary materials for an illustration of the task design). The n-back task followed a block design consisting of 0-back blocks and 2-back blocks presented in random order. There were four 0-back blocks and four 2-back blocks. Twenty seconds of resting blocks were presented between two neighboring task blocks. Six resting state blocks, with a total duration of 2 minutes, were concatenated as eyes-open resting state fMRI recordings (Fair et al., 2007). To minimize the impact of task-evoked responses on the resting state data, the first two volumes at the beginning of each resting state blocks were excluded, and the first two volumes of the following task block were included and assumed to be resting state.

Diffusion images, consisting of 64 weighted (b=1000s/mm^2) diffusion scans and 1 un-weighted (b=0 s/mm^2) scan, were recorded using a single-shot spin echo EPI sequence with the following parameters: field of view=256 mm×256 mm, matrix size=128×128, slice thickness=2 mm; each volume consisted of 73 axial slices. T1 image of 176 sagittal slices were recorded using a magnetization prepared rapid acquisition gradient-echo (MPRAGE) sequence with the following parameters: repetition time = 2500 ms, echo time = 3.77 ms, inversion time = 1050 ms, flip angle = 7 degrees, field of view=256mm×256mm, matrix = 256 × 256 and slice thickness=1 mm. T2 images of 176 sagittal slices were acquired using a Fluid Attenuated Inversion Recovery (FLAIR) sequence with following parameters: repetition time range across scans = 6000 ms, echo time = 395 ms and inversion time = 2100 ms.

EEG acquisition.: Scalp EEG data was separately recorded from 20 out of the 40 participants inside an acoustically and electrically shielded room with a 128-channel BioSemi Active Two System at a sampling rate of 1024 Hz. A left central posterior electrode served as reference. All participants went through 2 sessions of 2 min eyes-closed and 2 sessions of 2 min eyes-open resting states; the order of the sessions was randomized across participants.

2.3. Data Preprocessing

2.3.1. Young Dataset

EEG data.: Two sources of artifacts are specifically associated with EEG data acquired inside an MRI scanner: gradient and cardioballistic artifacts. The gradient artifact was removed by subtracting an average artifact template from the EEG data as implemented in Brain Vision Analyzer 2.0 (Brain Products GmbH). The gradient artifact template was constructed by using a sliding-window approach which involved averaging the EEG signal across 41 consecutive volumes. The cardioballistic artifact was removed by an average

artifact subtraction method proposed by (Allen et al., 1998). In this method, the R peaks were detected in the ECG recordings in a semiautomatic way and then utilized to construct a delayed average artifact template over 21 consecutive heartbeat events. The cardioballistic artifact was then removed by subtracting the average artifact templates from the EEG data. After these two steps, the EEG data were then bandpass filtered between 0.5 and 50Hz, down-sampled to 250 Hz, and re-referenced to the average reference. The MR-corrected EEG data were then exported to EEGLAB (Delorme & Makeig, 2004) to correct for eye-blinking, residual cardioballistic, and movement-related artifacts using ICA algorithms. Artifacts-corrected data were epoched into 1-second epochs and subjected to spectral analysis (see below).

FMRI data.: Functional MRI images, including eyes-closed and eyes-open resting state fMRI, were preprocessed according to the following steps. The first 5 functional scans of each session were discarded to eliminate the transient effects. The remaining fMRI images were preprocessed using SPM (http://www.fil.ion.ucl.ac.uk/spm/) which included the following steps: slice timing, motion correction, normalization to the Montreal Neurological Institute (MNI) template, and re-sampling of the functional images into a voxel size of $3\times3\times3$ mm^3 (Friston et al., 1995). Normalized images were spatially-smoothed by using a 7mm full width at half-maximum (FWHM) isotropic Gaussian kernel. Resting-state fMRI time series were then extracted from voxels within a gray matter brain mask after regressing out nine nuisance signals, including 6 movement variables and 3 averaged signals representing white matter, cerebral spinal fluid, and whole brain. These BOLD time series were then bandpass filtered between 0.01 and 0.1 Hz with a finite impulse response (FIR) filter. For each participant, a motion censoring procedure, called “motion scrubbing” (Power et al., 2012), was applied on the filtered BOLD signals to reduce the effects of transient movements on functional connectivity.

2.3.2. Old Dataset

EEG data.: Scalp EEG data preprocessing was performed off-line using BESA (http://www.besa.de/), EEGLAB (Delorme & Makeig, 2004) and custom scripts written in MATLAB. The protocol was similar to that of the young adults following MRI artifacts correction. Specifically, the original continuous data were bandpassed between 0.5 Hz and 50 Hz, down-sampled to 250 Hz, and epoched to 1-second epochs. Artifacts including eye movements and eye blinks, temporal muscle activity and line noise were removed from data epochs using ICA algorithms implemented in EEGLAB. Epochs with residual artifacts and with EEG activities exceeding 75 μV in any of the 128 scalp channels were excluded from further analysis. The remaining artifact-corrected signals were re-referenced to the average reference and subjected to spectral analysis (see below).

FMRI data.: Functional MRI images were analyzed using the same protocol as the young adults (see above).

Diffusion image.: Diffusion images were preprocessed by FMRIB’s diffusion toolbox (FDT), as part of FMRIB’s software library (FSL; http://www.fmrib.ox.ac.uk/fsl/). Standard DTI processing pipeline in FDT includes three steps of artifact controlling: 1) manual

removal of images affected by large artifacts, 2) eddy current correction, and 3) exclusion of non-brain areas by brain extraction tool (BET). Probability density functions with up to two principal fiber directions were estimated at each voxel on the diffusion data using the Bayesian estimation of diffusion parameters obtained using the sampling techniques toolbox (BEDPOSTX; (Behrens et al., 2007)) in FSL. For each individual, the first volume of diffusion image (b=0) was registered to standard MNI template via brain extracted T1 image, and brain extracted T2 image was also registered to T1 images, using FMRIB's linear image registration tool (FLIRT) implemented in FSL. The transformation matrix mapping diffusion space to standard MNI space and its inverse matrix were saved for following analysis. All registrations were visually inspected for aberrant registration.

2.4. Power Spectral Analysis of EEG Data

The scalp EEG voltage data from three occipital channels (O1, O2, and Oz) were employed for spectral power analysis (Mo et al., 2013; Strijkstra et al., 2003). Within each condition (EO versus EC), the power spectral density (PSD) of the occipital channels for each subject was estimated by applying the periodogram method to 1 s epochs of EEG data within the condition. For each occipital channel, Fourier transform was performed on the data from each epoch, and the amplitude was squared and averaged across all the epochs to yield PSD for that channel. Single channel PSD obtained this way was then averaged across the three occipital channels to yield the PSD for each subject within EC or EO condition. From each subject's PSD, alpha power was computed as the power within the frequency band of 8 to 12 Hz and alpha reactivity from EC to EO was defined as follows:

$$\text{alpha reactivity} = \frac{\text{EC alpha power} - \text{EO alpha power}}{\text{EC alpha power}}$$

According to this definition, the larger the alpha reactivity, the more the EC-to-EO alpha power decrease from EC to EO.

2.5. FMRI Functional Connectivity Analysis

The basal nucleus of Meynert (BNM) is a major source of cortical ACh (Johnston et al., 1981; Rye et al., 1984). To computer BNM-seeded functional connectivity, the BNM region of interest (ROI) was created based on a stereotaxic probability map of magnocellular cell groups in the basal forebrain, defined in the standard MNI space (Li et al., 2014; L. Zaborszky et al., 2008). For both Young Dataset and Old Dataset, taking the BNM ROI as the seed, BOLD signals from the seed region were averaged across seed voxels to yield one single BOLD signal representing BNM activity. Cross-correlation (CC) between the BNM BOLD signal and signals from all the other voxels in the gray matter mask of the brain was computed for each individual. The individual whole-brain correlation maps were converted to z-score maps by Fisher's z transformation. For each individual, an eyes-closed BNM-cortex functional connectivity map and an eyes-open BNM-cortex functional connectivity map were obtained by using eyes-closed and eyes-open resting state fMRI data, respectively. The resulting BNM-cortex functional connectivity maps were compared between EO and EC and subjected to a paired t-test across participants to obtain a t-value map quantifying the difference between BNM-cortex functional connectivity between eyes-closed and eyes-open

resting states. Visual cortex and anterior cingulate cortex (ACC) were identified as additional regions of interest (ROIs) because BNM-cortex functional connectivity maps in these regions showed significant difference ($p<0.05$, false discovery rate corrected) between eyes-closed and eyes-open resting states.

2.6. Measurement of Leukoaraiosis and Fiber Tracking

Leukoaraiosis (LA) is white-matter lesion prevalent in older adults and believed to have a role in disrupted neuronal communications (Bohnen & Albin, 2011). In MRI, LA manifests as hyper-intensity in FLAIR images. Past work shows that FLAIR protocols with semi-automated volumetrics have criterion validity relative to a LA visual rating scale (Price et al., 2012). For the Old Dataset, a reliable rater (inter-rater range: 0.84 – 0.93; intra-rater range > 0.99) measured all brain scans using in-house macros for ImageJ (http://rsbweb.nih.gov/ij/docs/index.html) (Abràmoff et al., 2004; Zijdenbos & Dawant, 1993). LA voxels for each brain slice were thresholded to create a 2D LA binary mask that were then concatenated into a 3D binary mask. This method also provided an estimate of total brain LA volume in mm^3.

Taking the basal nucleus of Meynert (BNM) as seed ROI (Li et al., 2014; Zaborszky et al., 2008) and the visual ROI and ACC ROI as two target ROIs, white matter fiber tracts were computed for the two ROI pairs: BNM-visual and BNM-ACC, using probabilistic tracking with crossing fibers (PROBTRACKX in FDT toolbox). Specifically, taking each voxel of BNM as seed, probabilistic tractography was performed to compute the probabilistic structural connectivity from the seed voxel to all the voxels within the target ROI. The probabilistic tractography algorithm stopped when the number of tracking steps exceeded 2000 or curvature threshold was larger than 0.2. For each individual, we initiated 5000 samples from structural connectivity distribution from each seed voxel to every target voxel, and the number of samples reaching one target voxel was defined as structural connectivity strength from the seed voxel. Individual probabilistic connectivity maps in diffusion space were realigned with individual T2-Flair image via T1 image and then overlaid on the 3D LA binary mask. The LA volume along BNM-visual and BNM-ACC tracts were obtained by counting the number of overlapping voxels.

3. RESULTS

3.1. Young Dataset

Alpha reactivity.—Occipital EEG traces were shown for both eyes-closed and eyes-open conditions in Figure 1a for one typical participant. At the group level, the average power spectra from the occipital channels were shown in Figure 1b, where the average alpha power under the eyes-closed condition is significantly higher than that under the eyes-open condition ($p < 0.001$). These results demonstrated the well-established alpha blocking or alpha desynchronization phenomenon initially described by Berger (Berger, 1933; Moosmann et al., 2003).

BNM-cortex functional connectivity.—The BNM ROI was shown in Figure 2a and was used as the seed for functional connectivity analysis. A paired t-test was applied to

compare BNM-seeded functional connectivity between the eyes-closed and eyes-open resting states. As shown in Figure 2b, compared with the eyes-closed condition, under the eyes-open state, BNM showed greater connectivity with the calcarine and middle occipital cortex, along with a set of other regions ($p<0.05$, uncorrected), including insular (INS) and inferior frontal gyrus (IFG).

Linking alpha reactivity and BNM-cortex functional connectivity.—We examined the relationship between the EC-to-EO alpha reactivity and the EC-to-EO BNM-visual functional connectivity change. The correlation, shown in Figure 2c, is statistically significant ($r = -0.389$, $p = 0.041$) according to a one-tailed test (Bauer et al., 2012; Bauml et al., 2008). The negative relationship suggests that the stronger the BNM-to-visual functional connectivity increase from EC to EO, the larger the EC-to-EO alpha reactivity.

3.2. Old Dataset

Alpha reactivity.—The power spectra averaged across participants were shown in Figure 3a. Similar to the young participants, the averaged alpha power under the eyes-closed condition was significantly higher than that under the eyes-open condition ($p < 0.001$), demonstrating the alpha-blocking or alpha desynchronization in older adults. Example time traces were shown in Figure 3b. Sample 1 was taken from a participant who exhibited clearly visible differences in alpha power under the eyes-closed and eyes-open conditions. Sample 2 represents a participant whose alpha power was not visibly different between eyes-closed and eyes-open states. Individual alpha reactivity for all subjects is shown in Figure 3c.

BNM-cortex functional connectivity.—The BNM-cortex functional connectivity maps were subjected to a paired t-test to examine the difference between eyes-closed and eyes-open states (Figure 4a). Defining ROIs as spheres 10 mm in diameter centered at the voxel with the strongest change in functional connectivity, we found two ROIs, one in visual cortex and the other in ACC, where BNM-cortex functional connectivity maps showed significant difference ($p < 0.05$, FDR). Compared to eyes-closed state, the ROI located in visual cortex (calcarine, middle and superior occipital cortex) showed significantly higher functional connectivity with the BNM in eyes-open resting, while the other ROI located in dorsal anterior cingulate cortex (ACC) showed significantly lower eyes-open state functional connectivity with BNM. Figure 4b shows that the BNM-visual functional connectivity difference was negatively correlated with the BNM-ACC functional connectivity difference ($r = -0.466$, $p = 0.044$). Namely, the more the BNM-visual functional connectivity increased from EC to EO, the more BNM-ACC functional connectivity decreased from EC to EO.

Linking alpha reactivity with BNM-cortex functional connectivity.—Consistent with the Young Dataset, the EC-to-EO BNM-visual functional connectivity difference was negatively correlated with alpha reactivity (Figure 4c; $r = -0.476$, $p = 0.039$), meaning that the stronger the BNM-visual functional connectivity increase from EC to EO, the larger the alpha reactivity from EC to EO. No correlation was found between BNM-ACC functional connectivity difference and alpha reactivity (Figure 4d; $r = 0.285$, $p = 0.237$).

Alpha reactivity and leukoaraiosis (LA).—Fiber tracts linking BNM and the visual ROI were shown in Figure 5a for a typical participant. Figure 5b shows the fiber tracts linking BNM and ACC from the same participant. The LA volume along the BNM-visual fiber tracts for each participant was calculated, and was found to be negatively correlated with alpha reactivity, as shown in Figure 5c ($r = -.459$, $p = 0.048$); namely, the higher the LA load, the weaker the alpha reactivity. The LA volume along the BNM-ACC fiber tracts was moderately correlated with alpha reactivity (Figure 5d; $r = -0.444$, $p = 0.057$). It was worth noting that the sum of LA volume along the BNM-visual and BNM-ACC fiber tracts was more correlated with alpha reactivity than the LA volume along each of the two tracts alone (Figure 5e; $r = -0.491$, $p = 0.033$). To test the robustness of the results, we further analyzed the data using the robust regression method (Rousseeuw & Leroy, 2005), and found that the three correlations in Figures 5c-5e became slightly weaker: BNM-visual LA vs alpha reactivity ($r = -0.433$, $p = 0.064$), BNM-ACC LA vs alpha reactivity ($r = -0.411$, $p = 0.080$), and LA along both tracts vs alpha reactivity ($r = -0.461$, $p = 0.047$).

4. DISCUSSION

Alpha power decrease from EC to EO is known as alpha blocking or alpha desynchronization. As indicated earlier, understanding the neural basis of this highly robust EEG phenomenon has both basic and clinical neuroscience significance. Defining alpha reactivity as the degree of alpha power decrease from EC to EO, we tested the role of acetylcholine (ACh), especially BNM and ACh pathways, in alpha blocking using a multimodal neuroimaging approach. Analyzing EEG and MRI data from a cohort of young adults and a cohort of cognitively well older adults we reported two main findings. First, BNM connectivity to visual cortex was increased from EC to EO, and this increase was positively associated with alpha reactivity in both young and older adults, namely, the stronger the BNM-visual functional connectivity increase from EC to EO, the larger the alpha power decreased from EC to EO (i.e., larger alpha reactivity). Second, in older adults, LA load along BNM-visual cortex white matter fiber tracts negatively associated with alpha reactivity, namely, the higher the LA load along the BNM-visual fiber tracts, the smaller the alpha reactivity.

EEG desynchronization signifies cortical activation and behavioral arousal (Jasper & Carmichael, 1935). From eyes-closed resting to eyes-open resting, EEG undergoes such activation/desynchronization transition. A possible role of acetylcholine in modulating EC to EO differences in EEG was initially suggested in animal studies. In vivo microdialysis in rats shows that the presentation of sensory stimuli increased acetylcholine release in both the hippocampus and cortex, which is consistent with a role of acetylcholine in arousal and attention (Inglis & Fibiger, 1995). Anatomically, the basal nucleus of Meynert (BNM) of the basal forebrain is the primary source of cortical ACh (Johnston et al., 1981; Rye et al., 1984). A number of studies indicate a relationship between BNM activity, ACh, and arousal. The discharge rate of BNM neurons is reported to vary with the degree of EEG activation: greater BNM activity is associated with more EEG activation (Buzsaki et al., 1988; Detari & Vanderwolf, 1987). Also, excitotoxic BNM lesions or systemic administration of muscarinic cholinergic receptor antagonists renders the cortical EEG resistant to desynchronization in awake animals (Buzsaki et al., 1988; Stewart et al., 1984). Furthermore, stimulation of the

BNM results in cortical ACh release and EEG activation/desynchronization (Belardetti et al., 1977; Casamenti et al., 1986; Metherate & Ashe, 1991). To what extent these results generalize to humans is what we addressed in this study.

Direct perturbation of the brain's cholinergic system in humans is difficult. Past work has used cholinergic drugs to manipulate the level of acetylcholine (Bauer et al., 2012; Meador et al., 1989; Silver et al., 2008). However, cholinergic drugs have systemic effects that are not limited to the brain; moreover, these drugs can have adverse effects, particularly in the older population. Numerous neuroimaging studies have suggested functional connectivity analysis based on resting-state fMRI data as a useful alternative to characterize the role of a brain region such as BNM (Biswal et al., 1995; Fair et al., 2007; Fox & Raichle, 2007). Assuming that the role of acetylcholine in EO and EC alpha reactivity can be inferred from such an analysis applied to EO and EC resting state fMRI and EEG data, we found that, in both the Young and Old Datasets, the BNM and visual cortex were more functionally connected during eyes-open relative to eyes-closed. We interpreted this functional connectivity change as indicative of increased projection of acetylcholine from the BNM to visual cortex from EC to EO. If our interpretation is accurate, namely, cortical activation associated with EO is mediated by increased activity of cholinergic neurons that project their outputs to the visual cortex, then our results are broadly in line with the animal studies cited above (Inglis & Fibiger, 1995). In addition, relevant for the main topic of this study, the BNM-visual cortex functional connectivity increase from EC to EO predicted alpha reactivity from EC to EO in both datasets, thereby demonstrating a role of BNM and associated cholinergic pathways in alpha reactivity.

Leukoaraiosis (LA) is a naturally occurring lesion prevalent in the white matter of older adults and is often attributed to changes within the supportive smaller arterioles supplying the white matter (Longstreth et al., 1996; Pantoni & Garcia, 1995). Our finding that the higher the LA load along the BNM-visual cortex fiber tracts, the less the alpha reactivity suggests that disrupting neuronal transmissions from BNM to visual cortex can lead to reduced alpha reactivity in older participants. (It is worth noting that this effect is quite specific in that there was no significant correlation between the whole brain LA volume and alpha reactivity ($r = -0.348$, $p = 0.144$)). This result provides causal evidence that ACh pathways, and indirectly ACh itself, play a vital role in modulating EC-to-EO alpha reactivity. The clinical relevance of these findings lies in that previous studies suggest loss of neurons in the basal forebrain provides a pathological substrate for the cholinergic deficiency in patients with Alzheimer's disease (Whitehouse et al., 1982), and a high percentage of AD patients show evidence of increased LA and lower alpha reactivity comparing to normal controls (Brown et al., 2000; Moretti et al., 2004).

One notable difference between young and older cohorts is that in the older cohort BNM-ACC functional connectivity, which manifested as negative correlations, was different between EC and EO; it was smaller in magnitude in EO than in EC, and the difference has an apparently positive but statistically insignificant correlation with alpha reactivity. In the young cohort, no BNM-ACC functional connectivity difference between EC and EO resting states was observed. Attempting to explain this observation, we note that in a non-human primate study, it has been suggested that anterior cingulate cortex was a critical region in

cholinergic modulation, exerting inhibitory cholinergic influence via m2 cholinergic receptors (Medalla & Barbas, 2012). There is further evidence that BNM inhibits frontal cortex via GABAergic projections (Ballinger et al., 2016). We speculate that the negative BNM-ACC correlation may stem partly from the mutual inhibition between ACC and BNM (Chen et al., 2011; Goelman et al., 2014). Reduced BNM-ACC functional connectivity magnitude during EO may reflect reduced inhibition of BNM, which then gives rise to increased ACh projections from BNM to visual cortex, a scenario consistent with the pattern observed in Figure 4b. Aging's role in cortical acetylcholine has been studied in rodent models (Sarter & Bruno, 1998). Compared to young rats, the activity of cortical choline acetyltransferase (ChAT), an important marker of cortical acetylcholine, was found to be significantly decreased in ACC in aged rats (Biegon et al., 1986). Such age-related changes may underlie the observed difference in BNM-ACC functional connectivity between the young and older cohorts. Interestingly, there was a moderate association between alpha reactivity and LA load along the BNM to ACC fiber tracts, although the fiber tracts linking BNM with visual cortex and that linking BNM with ACC belong to different major cholinergic pathways (Selden et al., 1998), further suggesting that BNM-ACC interactions have implications for alpha reactivity. Other evidence linking ACC and alpha oscillations includes: Resting state BOLD activities in ACC was found to be negatively correlated with posterior alpha power (Laufs et al., 2003) and posterior alpha power difference between EC and EO during resting state was negatively correlated with hemodynamic responses and inter-regional functional connectivity in ACC (Wu et al., 2010; Yu et al., 2016).

This study has limitations. First, the two datasets analyzed were derived from separate investigations and recruitment procedures. This may have introduced bias into the participant selection process. Second, procedurally, the young adults underwent an EEG-fMRI simultaneous recording, but not diffusion recording, while the older adults had diffusion recording, but separate EEG and fMRI sessions. This may have introduced bias in the data acquisition process. Third, extracting eyes-open resting state BOLD signals from the resting blocks placed between task blocks in the n-back tasks may present problems. Although we took steps to minimize the impact of task-evoked activities of the preceding task block on resting state data, task-evoked responses may not be eliminated from resting state blocks. Moreover, past work has shown that BOLD signals can be affected by a prior task even minutes after the cessation of the task (Bolt et al., 2018; Yao et al., 2007). Fourth, some of the interpretations above are quite speculative owing to the dearth of knowledge in this area, which is partly attributable to our lack of the ability to directly manipulate pertinent variables in noninvasive human imaging. Future work utilizing animal preparations in addition to human subjects will be essential to validate and substantiate the findings reported here.

5. CONCLUSION

This study demonstrated a role of BNM, cholinergic pathways and indirectly ACh itself, in modulating a salient aspect of resting-state alpha oscillations, namely, its EC-to-EO reactivity. Instead of systemically manipulating the level of ACh using pharmacological means, as has been done in past studies, we utilized the recently published mask for BNM and indexed the impact of cholinergic activation using BNM-cortex functional connectivity

and naturally occurring lesions. In both young and older adults, BNM-visual functional connectivity was shown to be increased from EC to EO, and this increase predicted alpha reactivity. Lesion data in older adults further provide causal evidence supporting a role of BNM and cholinergic pathways in modulating alpha reactivity.

Supplementary Material

Refer to Web version on PubMed Central for supplementary material.

ACKNOWLEDGMENTS

This work was supported by the National Institutes of Health (NIH) grants R01 NR014181, R01 NS082386, R01 NR014810 and R01 MH117991, and National Science Foundation grant BCS-1344285. The authors declare no conflicts of interest.

REFERENCES

Abràmoff MD, Magalhães PJ, & Ram SJ (2004). Image processing with ImageJ. Biophotonics international, 11(7), 36–42.

Adrian ED, & Matthews B (1934). The interpretation of potential waves in the cortex. The Journal of Physiology, 81(4), 440–471. 10.1113/jphysiol.1934.sp003147 [PubMed: 16994555]

Allen PJ, Polizzi G, Krakow K, Fish DR, & Lemieux L (1998). Identification of EEG events in the MR scanner: the problem of pulse artifact and a method for its subtraction. Neuroimage, 8(3), 229–239. 10.1006/nimg.1998.0361 [PubMed: 9758737]

Association, A. P. (2000). Diagnostic and Statistical Manual of Mental Disorders, revised Washington DC: American Psychiatric Association, 943, 2000 10.1176/appi.books.9780890425596

Babiloni C, Lizio R, Vecchio F, Frisoni GB, Pievani M, Geroldi C, . . . Rossini PM (2010). Reactivity of cortical alpha rhythms to eye opening in mild cognitive impairment and Alzheimer's disease: an EEG study. Journal of Alzheimer's Disease, 22(4), 1047–1064. 10.3233/JAD-2010-100798

Ballinger EC, Ananth M, Talmage DA, & Role LW (2016). Basal Forebrain Cholinergic Circuits and Signaling in Cognition and Cognitive Decline. Neuron, 91(6), 1199–1218. 10.1016/j.neuron.2016.09.006 [PubMed: 27657448]

Barber M, & Stott DJ (2004). Validity of the Telephone Interview for Cognitive Status (TICS) in post-stroke subjects. International journal of geriatric psychiatry, 19(1), 75–79. 10.1002/gps.1041 [PubMed: 14716702]

Bauer M, Kluge C, Bach D, Bradbury D, Heinze HJ, Dolan RJ, & Driver J (2012). Cholinergic enhancement of visual attention and neural oscillations in the human brain. Curr Biol, 22(5), 397–402. 10.1016/j.cub.2012.01.022 [PubMed: 22305751]

Bauml KH, Hanslmayr S, Pastotter B, & Klimesch W (2008). Oscillatory correlates of intentional updating in episodic memory. Neuroimage, 41(2), 596–604. 10.1016/j.neuroimage.2008.02.053 [PubMed: 18420423]

Behrens TE, Berg HJ, Jbabdi S, Rushworth MF, & Woolrich MW (2007). Probabilistic diffusion tractography with multiple fibre orientations: What can we gain? Neuroimage, 34(1), 144–155. 10.1016/j.neuroimage.2006.09.018 [PubMed: 17070705]

Belardetti F, Borgia R, & Mancia M (1977). Prosencephalic mechanisms of ECoG desynchronization in cerveau isole cats. Electroencephalogr Clin Neurophysiol, 42(2), 213–225. 10.1016/0013-4694(77)90028-1 [PubMed: 65257]

Berger H (1933). Über das elektrenkephalogramm des menschen. European archives of psychiatry and clinical neuroscience, 98(1), 231–254. 10.1007/BF01797193

Biegon A, Greenberger V, & Segal M (1986). Quantitative histochemistry of brain acetylcholinesterase and learning rate in the aged rat. Neurobiol Aging, 7(3), 215–217. 10.1016/0197-4580(86)90046-1 [PubMed: 3724956]

Biswal B, Zerrin Yetkin F, Haughton VM, & Hyde JS (1995). Functional connectivity in the motor cortex of resting human brain using echo-planar mri. Magnetic resonance in medicine, 34(4), 537–541. 10.1002/mrm.1910340409 [PubMed: 8524021]

Bohnen NI, & Albin RL (2011). White matter lesions in Parkinson disease. Nat Rev Neurol, 7(4), 229–236. 10.1038/nrneurol.2011.21 [PubMed: 21343896]

Bolt T, Anderson ML, & Uddin LQ (2018). Beyond the evoked/intrinsic neural process dichotomy. Netw Neurosci, 2(1), 1–22. 10.1162/NETN_a_00028 [PubMed: 29911670]

Breteler MM, van Amerongen NM, van Swieten JC, Claus JJ, Grobbee DE, van Gijn J, . . . van Harskamp F. (1994). Cognitive correlates of ventricular enlargement and cerebral white matter lesions on magnetic resonance imaging. The Rotterdam Study. Stroke, 25(6), 1109–1115. 10.1161/str.25.6.8202966 [PubMed: 8202966]

Brown WR, Moody DM, Thore CR, & Challa VR (2000). Cerebrovascular pathology in Alzheimer's disease and leukoaraiosis. Ann N Y Acad Sci, 903(1), 39–45. 10.1111/j.1749-6632.2000.tb06348.x [PubMed: 10818487]

Buzsaki G, Bickford RG, Ponomareff G, Thal LJ, Mandel R, & Gage FH (1988). Nucleus basalis and thalamic control of neocortical activity in the freely moving rat. J Neurosci, 8(11), 4007–4026. 10.1523/JNEUROSCI.08-11-04007.1988 [PubMed: 3183710]

Casamenti F, Deffenu G, Abbamondi AL, & Pepeu G (1986). Changes in cortical acetylcholine output induced by modulation of the nucleus basalis. Brain Res Bull, 16(5), 689–695. 10.1016/0361-9230(86)90140-1 [PubMed: 3742251]

Chapman RM, Armington JC, & Bragdon HR (1962). A quantitative survey of kappa and alpha EEG activity. Electroencephalogr Clin Neurophysiol, 14(6), 858–868. 10.1016/0013-4694(62)90136-0 [PubMed: 14020161]

Chen G, Chen G, Xie C, & Li SJ (2011). Negative functional connectivity and its dependence on the shortest path length of positive network in the resting-state human brain. Brain Connect, 1(3), 195–206. 10.1089/brain.2011.0025 [PubMed: 22433048]

Li CS, Ide JS, Zhang S, Hu S, Chao HH, & Zaborszky L (2014). Resting state functional connectivity of the basal nucleus of Meynert in humans: In comparison to the ventral striatum and the effects of age. Neuroimage, 97, 321–332. 10.1016/j.neuroimage.2014.04.019 [PubMed: 24736176]

Delorme A, & Makeig S (2004). EEGLAB: an open source toolbox for analysis of single-trial EEG dynamics including independent component analysis. Journal of neuroscience methods, 134(1), 9–21. 10.1016/j.jneumeth.2003.10.009 [PubMed: 15102499]

Detari L, & Vanderwolf CH (1987). Activity of identified cortically projecting and other basal forebrain neurones during large slow waves and cortical activation in anaesthetized rats. Brain Res, 437(1), 1–8. 10.1016/0006-8993(87)91521-6 [PubMed: 2827860]

Duffy FH, Albert MS, McAnulty G, & Garvey AJ (1984). Age-related differences in brain electrical activity of healthy subjects. Annals of neurology, 16(4), 430–438. 10.1002/ana.410160403 [PubMed: 6497352]

Fair DA, Schlaggar BL, Cohen AL, Miezin FM, Dosenbach NU, Wenger KK, . . . Petersen SE (2007). A method for using blocked and event-related fMRI data to study "resting state" functional connectivity. Neuroimage, 35(1), 396–405. 10.1016/j.neuroimage.2006.11.051 [PubMed: 17239622]

Feige B, Scheffler K, Esposito F, Di Salle F, Hennig J, & Seifritz E (2005). Cortical and subcortical correlates of electroencephalographic alpha rhythm modulation. J Neurophysiol, 93(5), 2864–2872. 10.1152/jn.00721.2004 [PubMed: 15601739]

Fox MD, & Raichle ME (2007). Spontaneous fluctuations in brain activity observed with functional magnetic resonance imaging. Nature reviews neuroscience, 8(9), 700–711. 10.1038/nrn2201 [PubMed: 17704812]

Friston K, Ashburner J, Frith CD, Poline JB, Heather JD, & Frackowiak RS (1995). Spatial registration and normalization of images. Human brain mapping, 3(3), 165–189. 10.1002/hbm.460030303

Gale A, Coles M, & Boyd E (1971). Variation in visual input and the occipital EEG: II. Psychonomic Science, 23(1), 99–100. 10.3758/BF03336026

Glass A, & Kwiatkowski AW (1970). Power spectral density changes in the EEG during mental arithmetic and eye-opening. Psychol Forsch, 33(2), 85–99. 10.1007/BF00424979 [PubMed: 5515904]

Goard M, & Dan Y (2009). Basal forebrain activation enhances cortical coding of natural scenes. Nat Neurosci, 12(11), 1444–1449. 10.1038/nn.2402 [PubMed: 19801988]

Goelman G, Gordon N, & Bonne O (2014). Maximizing negative correlations in resting-state functional connectivity MRI by time-lag. PloS one, 9(11), e111554 10.1371/journal.pone.0111554 [PubMed: 25396416]

Hachinski VC, Potter P, & Merskey H (1987). Leuko-araiosis. Archives of neurology, 44(1), 21–23. 10.1001/archneur.1987.00520130013009 [PubMed: 3800716]

Hanslmayr S, Sauseng P, Doppelmayr M, Schabus M, & Klimesch W (2005). Increasing individual upper alpha power by neurofeedback improves cognitive performance in human subjects. Applied psychophysiology and biofeedback, 30(1), 1–10. 10.1007/s10484-005-2169-8 [PubMed: 15889581]

Hardle W, Gasser T, & Bacher P (1984). EEG-responsiveness to eye opening and closing in mildly retarded children compared to a control group. Biol Psychol, 18(3), 185–199. 10.1016/0301-0511(84)90002-4 [PubMed: 6743728]

Hogervorst E, Ribeiro HM, Molyneux A, Budge M, & Smith AD (2002). Plasma homocysteine levels, cerebrovascular risk factors, and cerebral white matter changes (leukoaraiosis) in patients with Alzheimer disease. Archives of neurology, 59(5), 787–793. 10.1001/archneur.59.5.787 [PubMed: 12020261]

Inglis F, & Fibiger H (1995). Increases in hippocampal and frontal cortical acetylcholine release associated with presentation of sensory stimuli. Neuroscience, 66(1), 81–86. 10.1016/0306-4522(94)00578-S [PubMed: 7637877]

Jasper HH (1936). Cortical Excitatory State and Variability in Human Brain Rhythms. science, 83(2150), 259–260. 10.1126/science.83.2150.259 [PubMed: 17757098]

Jasper HH, & Carmichael L (1935). Electrical potentials from the intact human brain. science. 10.1126/science.81.2089.51

Johnston MV, McKinney M, & Coyle JT (1981). Neocortical cholinergic innervation: a description of extrinsic and intrinsic components in the rat. Exp Brain Res, 43(2), 159–172. 10.1007/BF00237760 [PubMed: 6265265]

Laufs H, Kleinschmidt A, Beyerle A, Eger E, Salek-Haddadi A, Preibisch C, & Krakow K (2003). EEG-correlated fMRI of human alpha activity. Neuroimage, 19(4), 1463–1476. 10.1016/S1053-8119(03)00286-6 [PubMed: 12948703]

Legewie H, Simonova O, & Creutzfeldt O (1969). EEG changes during performance of various tasks under open-and closed-eyed conditions. Electroencephalography and clinical neurophysiology, 27(5), 470–479. 10.1016/0013-4694(69)90187-4 [PubMed: 4187033]

Longstreth WT, Jr., Manolio TA, Arnold A, Burke GL, Bryan N, Jungreis CA, . . . Fried L (1996). Clinical correlates of white matter findings on cranial magnetic resonance imaging of 3301 elderly people. The Cardiovascular Health Study. Stroke, 27(8), 1274–1282. 10.1159/000026235 [PubMed: 8711786]

McBride JC, Zhao X, Munro NB, Smith CD, Jicha GA, Hively L, . . . Jiang Y (2014). Spectral and complexity analysis of scalp EEG characteristics for mild cognitive impairment and early Alzheimer's disease. Computer methods and programs in biomedicine, 114(2), 153–163. 10.1016/j.cmpb.2014.01.019 [PubMed: 24598317]

Meador KJ, Loring DW, Davis HC, Sethi KD, Patel BR, Adams RJ, & Hammond EJ (1989). Cholinergic and serotonergic effects on the P3 potential and recent memory. J Clin Exp Neuropsychol, 11(2), 252–260. 10.1080/01688638908400887 [PubMed: 2925834]

Medalla M, & Barbas H (2012). The anterior cingulate cortex may enhance inhibition of lateral prefrontal cortex via m2 cholinergic receptors at dual synaptic sites. Journal of Neuroscience, 32(44), 15611–15625. 10.1523/JNEUROSCI.2339-12.2012 [PubMed: 23115196]

Metherate R, & Ashe JH (1991). Basal forebrain stimulation modifies auditory cortex responsiveness by an action at muscarinic receptors. Brain research, 559(1), 163–167. 10.1016/0006-8993(91)90301-B [PubMed: 1782557]

Metherate R, Cox CL, & Ashe JH (1992). Cellular bases of neocortical activation: modulation of neural oscillations by the nucleus basalis and endogenous acetylcholine. J Neurosci, 12(12), 4701–4711. 10.1523/JNEUROSCI.12-12-04701.1992 [PubMed: 1361197]

Mintzer J, & Burns A (2000). Anticholinergic side-effects of drugs in elderly people. J R Soc Med, 93(9), 457–462. 10.1177/014107680009300903 [PubMed: 11089480]

Mo J, Liu Y, Huang H, & Ding M (2013). Coupling between visual alpha oscillations and default mode activity. Neuroimage, 68, 112–118. 10.1016/j.neuroimage.2012.11.058 [PubMed: 23228510]

Moosmann M, Ritter P, Krastel I, Brink A, Thees S, Blankenburg F, . . . Villringer A (2003). Correlates of alpha rhythm in functional magnetic resonance imaging and near infrared spectroscopy. Neuroimage, 20(1), 145–158. 10.1016/S1053-8119(03)00344-6 [PubMed: 14527577]

Moretti DV, Babiloni C, Binetti G, Cassetta E, Dal Forno G, Ferreric F, . . . Rossini PM (2004). Individual analysis of EEG frequency and band power in mild Alzheimer's disease. Clin Neurophysiol, 115(2), 299–308. 10.1016/S1388-2457(03)00345-6 [PubMed: 14744569]

Mufson EJ, Ginsberg SD, Ikonomovic MD, & DeKosky ST (2003). Human cholinergic basal forebrain: chemoanatomy and neurologic dysfunction. J Chem Neuroanat, 26(4), 233–242. 10.1016/S0891-0618(03)00068-1 [PubMed: 14729126]

Muir JL, Page KJ, Sirinathsinghji D, Robbins TW, & Everitt BJ (1993). Excitotoxic lesions of basal forebrain cholinergic neurons: effects on learning, memory and attention. Behavioural brain research, 57(2), 123–131. 10.1016/0166-4328(93)90128-D [PubMed: 7509608]

Pantoni L, & Garcia JH (1995). The significance of cerebral white matter abnormalities 100 years after Binswanger's report a review. Stroke, 26(7), 1293–1301. 10.1161/str.26.7.1293 [PubMed: 7604429]

Pantoni L, & Garcia JH (1997). Pathogenesis of leukoaraiosis: a review. Stroke, 28(3), 652–659. [PubMed: 9056627]

Power JD, Barnes KA, Snyder AZ, Schlaggar BL, & Petersen SE (2012). Spurious but systematic correlations in functional connectivity MRI networks arise from subject motion. Neuroimage, 59(3), 2142–2154. 10.1016/j.neuroimage.2011.10.018 [PubMed: 22019881]

Price CC, Mitchell SM, Brumback B, Tanner JJ, Schmalfuss I, Lamar M, . . . Libon DJ (2012). MRI-leukoaraiosis thresholds and the phenotypic expression of dementia. Neurology, 79(8), 734–740. 10.1212/WNL.0b013e3182661ef6 [PubMed: 22843264]

Price CC, Tanner JJ, Schmalfuss IM, Brumback B, Heilman KM, & Libon DJ (2015). Dissociating Statistically-Determined Alzheimer's Disease/Vascular Dementia Neuropsychological Syndromes Using White and Gray Neuroradiological Parameters. Journal of Alzheimer's Disease, 48(3), 833–847. 10.3233/JAD-150407

Raghanti M-A, Simic G, Watson S, Stimpson CD, Hof PR, & Sherwood CC (2011). Comparative analysis of the nucleus basalis of Meynert among primates. Neuroscience, 184, 1–15. 10.1016/j.neuroscience.2011.04.008 [PubMed: 21504783]

Richardson RT, & DeLong MR (1988). A reappraisal of the functions of the nucleus basalis of Meynert. Trends Neurosci, 11(6), 264–267. 10.1016/0166-2236(88)90107-5 [PubMed: 2465623]

Rousseeuw PJ, & Leroy AM (2005). Robust regression and outlier detection (Vol. 589): John wiley & sons 10.1002/0471725382

Rudolph JL, Salow MJ, Angelini MC, & McGlinchey RE (2008). The anticholinergic risk scale and anticholinergic adverse effects in older persons. Arch Intern Med, 168(5), 508–513. 10.1001/archinternmed.2007.106 [PubMed: 18332297]

Rye DB, Wainer BH, Mesulam MM, Mufson EJ, & Saper CB (1984). Cortical projections arising from the basal forebrain: a study of cholinergic and noncholinergic components employing combined retrograde tracing and immunohistochemical localization of choline acetyltransferase. Neuroscience, 13(3), 627–643. 10.1016/0306-4522(84)90083-6 [PubMed: 6527769]

Sarter M, & Bruno JP (1998). Age-related changes in rodent cortical acetylcholine and cognition: main effects of age versus age as an intervening variable. Brain research reviews, 27(2), 143–156. 10.1016/S0165-0173(98)00003-4 [PubMed: 9622614]

Schmidt R, Fazekas F, Kapeller P, Schmidt H, & Hartung H-P (1999). MRI white matter hyperintensities Three-year follow-up of the Austrian Stroke Prevention Study. Neurology, 53(1), 132–132. 10.1212/WNL.53.1.132 [PubMed: 10408549]

Selden NR, Gitelman DR, Salamon-Murayama N, Parrish TB, & Mesulam M-M (1998). Trajectories of cholinergic pathways within the cerebral hemispheres of the human brain. Brain, 121(12), 2249–2257. 10.1093/brain/121.12.2249 [PubMed: 9874478]

Silver MA, Shenhav A, & D'Esposito M (2008). Cholinergic enhancement reduces spatial spread of visual responses in human early visual cortex. Neuron, 60(5), 904–914. 10.1016/j.neuron.2008.09.038 [PubMed: 19081383]

Smith JR (1938). The electroencephalogram during normal infancy and childhood: II. The nature of the growth of the alpha waves. The Pedagogical Seminary and Journal of Genetic Psychology, 53(2), 455–469. 10.1080/08856559.1938.10533821

Stewart DJ, Macfabe DF, & Vanderwolf C (1984). Cholinergic activation of the electrocorticogram: role of the substantia innominata and effects of atropine and quinuclidinyl benzilate. Brain research, 322(2), 219–232. 10.1016/0006-8993(84)90112-4 [PubMed: 6509315]

Strijkstra AM, Beersma DG, Drayer B, Halbesma N, & Daan S (2003). Subjective sleepiness correlates negatively with global alpha (8–12 Hz) and positively with central frontal theta (4–8 Hz) frequencies in the human resting awake electroencephalogram. Neuroscience letters, 340(1), 17–20. 10.1016/S0304-3940(03)00033-8 [PubMed: 12648748]

Thiele A (2009). Optimizing brain processing. Nat Neurosci, 12(11), 1359–1360. 10.1038/nn1109-1359 [PubMed: 19861947]

Volavka J, Matousek M, & Roubicek J (1967). Mental arithmetic and eye opening. An EEG frequency analysis and GSR study. Electroencephalogr Clin Neurophysiol, 22(2), 174–176. 10.1016/0013-4694(67)90158-7 [PubMed: 4163688]

Voytko ML, Olton DS, Richardson RT, Gorman LK, Tobin JR, & Price DL (1994). Basal forebrain lesions in monkeys disrupt attention but not learning and memory [published erratum appears in J Neurosci 1995 Mar; 15 (3): following table of contents]. Journal of Neuroscience, 14(1), 167–186. 10.1523/JNEUROSCI.14-01-00167.1994 [PubMed: 8283232]

Wenk GL (1997). The nucleus basalis magnocellularis cholinergic system: one hundred years of progress. Neurobiol Learn Mem, 67(2), 85–95. 10.1006/nlme.1996.3757 [PubMed: 9075237]

Whitehouse PJ, Price DL, Struble RG, Clark AW, Coyle JT, & Delon MR (1982). Alzheimer's disease and senile dementia: loss of neurons in the basal forebrain. science, 215(4537), 1237–1239. 10.1126/science.7058341 [PubMed: 7058341]

Wu L, Eichele T, & Calhoun VD (2010). Reactivity of hemodynamic responses and functional connectivity to different states of alpha synchrony: a concurrent EEG-fMRI study. Neuroimage, 52(4), 1252–1260. 10.1016/j.neuroimage.2010.05.053 [PubMed: 20510374]

Yao H, Shi L, Han F, Gao H, & Dan Y (2007). Rapid learning in cortical coding of visual scenes. Nat Neurosci, 10(6), 772–778. 10.1038/nn1895 [PubMed: 17468750]

Ylikoski R, Ylikoski A, Erkinjuntti T, Sulkava R, Raininko R, & Tilvis R (1993). White matter changes in healthy elderly persons correlate with attention and speed of mental processing. Archives of neurology, 50(8), 818–824. 10.1001/archneur.1993.00540080029009 [PubMed: 8352667]

Yu Q, Wu L, Bridwell DA, Erhardt EB, Du Y, He H, . . . Calhoun VD (2016). Building an EEG-fMRI Multi-Modal Brain Graph: A Concurrent EEG-fMRI Study. Front Hum Neurosci, 10, 476 10.3389/fnhum.2016.00476 [PubMed: 27733821]

Zaborszky L, Csordas A, Mosca K, Kim J, Gielow MR, Vadasz C, & Nadasdy Z (2015). Neurons in the basal forebrain project to the cortex in a complex topographic organization that reflects corticocortical connectivity patterns: an experimental study based on retrograde tracing and 3D reconstruction. Cerebral cortex, 25(1), 118–137. 10.1093/cercor/bht210 [PubMed: 23964066]

Zaborszky L, Hoemke L, Mohlberg H, Schleicher A, Amunts K, & Zilles K (2008). Stereotaxic probabilistic maps of the magnocellular cell groups in human basal forebrain. Neuroimage, 42(3), 1127–1141. 10.1016/j.neuroimage.2008.05.055 [PubMed: 18585468]

Zaborszky L, van den Pol A, & Gyengesi E (2012). The basal forebrain cholinergic projection system in mice. The Mouse Nervous System, 28, 684–718. 10.1016/B978-0-12-369497-3.10028-7

Zijdenbos AP, & Dawant BM (1993). Brain segmentation and white matter lesion detection in MR images. Critical reviews in biomedical engineering, 22(5–6), 401–465.

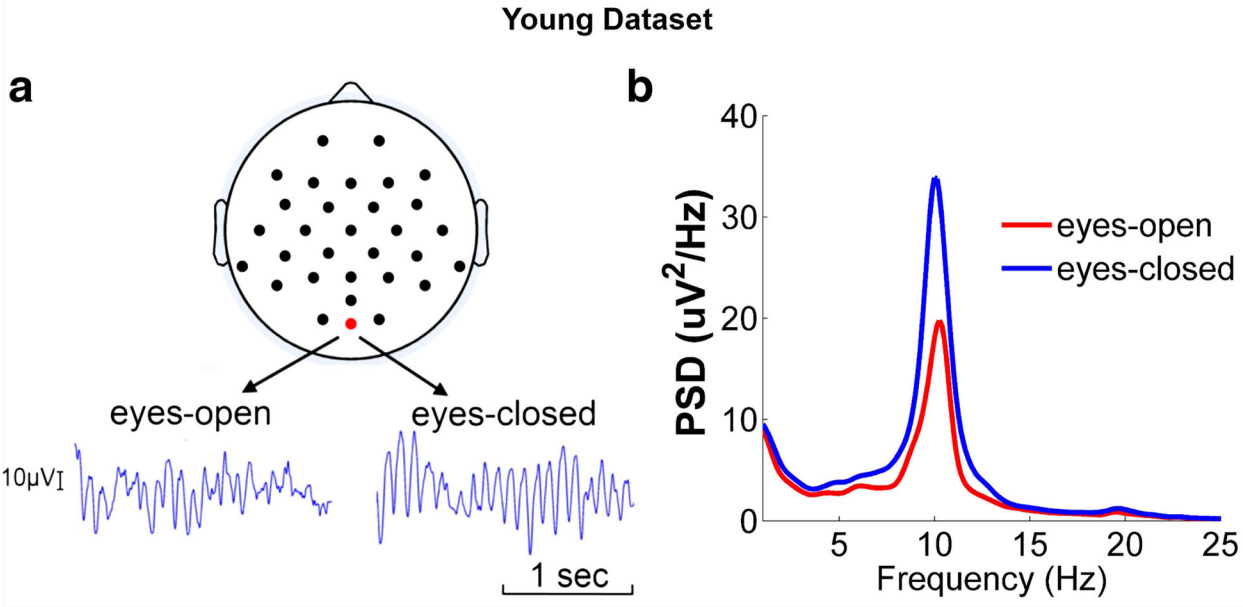

FIGURE 1. Alpha oscillations during EC and EO resting state in young adults.
(a) EEG traces of a typical participant. (b) Power spectra averaged across participants.

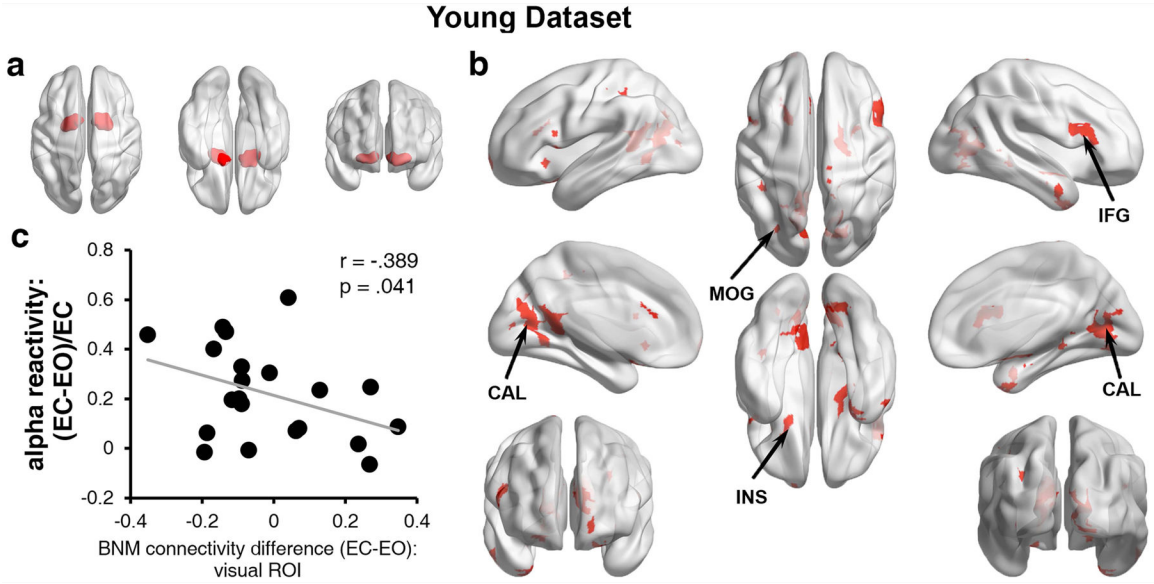

FIGURE 2. BNM-seeded functional connectivity and alpha reactivity for young adults.

(a) Basal nucleus of Meynert (BNM) region of interest. (b) Brain areas showing increased (warm color) and decreased (none) functional connectivity to BNM from the EC to EO state ($p<0.05$, uncorrected). (c) EC-to-EO alpha reactivity was significantly associated with the EC-to-EO difference in BNM-visual functional connectivity. MOG: middle occipital gyrus; CAL: calcarine; IFG: inferior frontal gyrus; INS: insula.

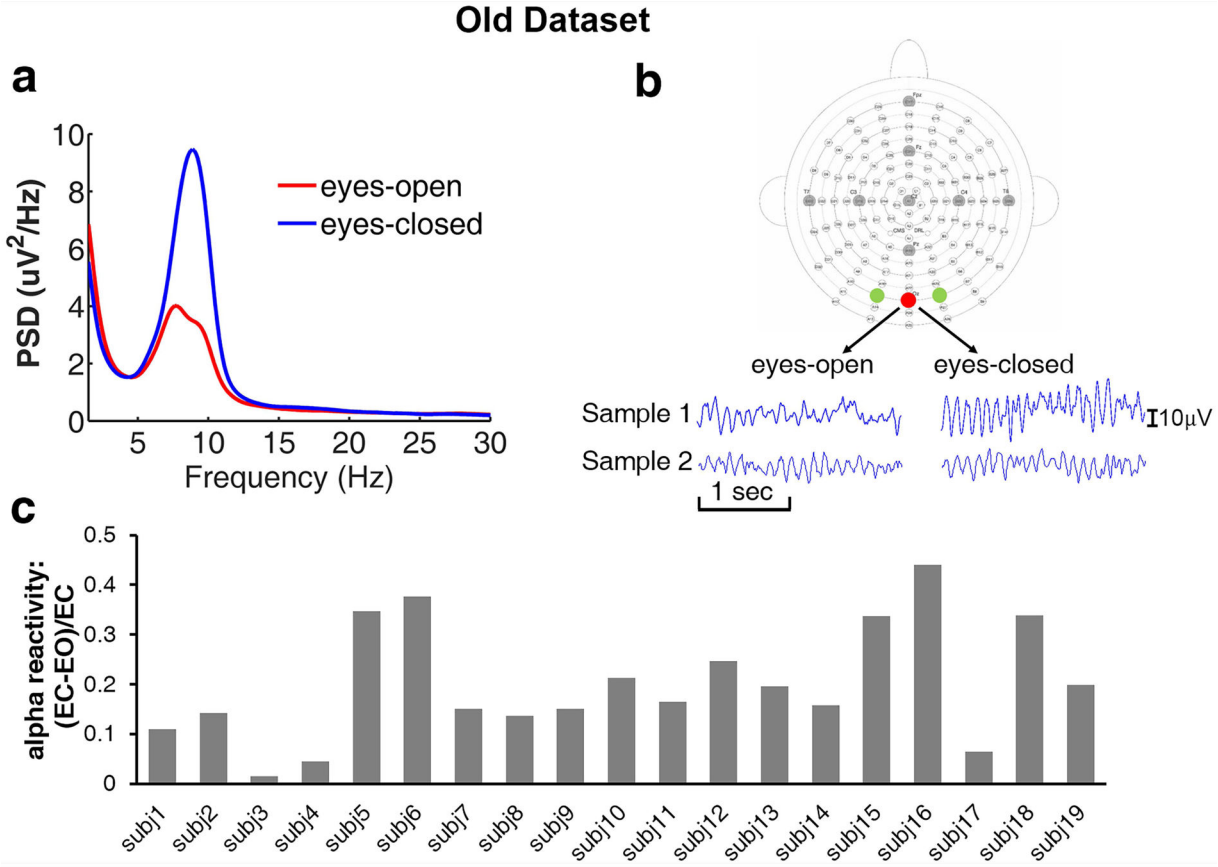

FIGURE 3. Alpha oscillations during EC and EO resting state in older adults.

(a) Power spectra from occipital channels averaged across participants. (b) Two participants showing strong (sample 1) and weak (sample 2) alpha reactivity. (c) Individual EC-to-EO alpha reactivity.

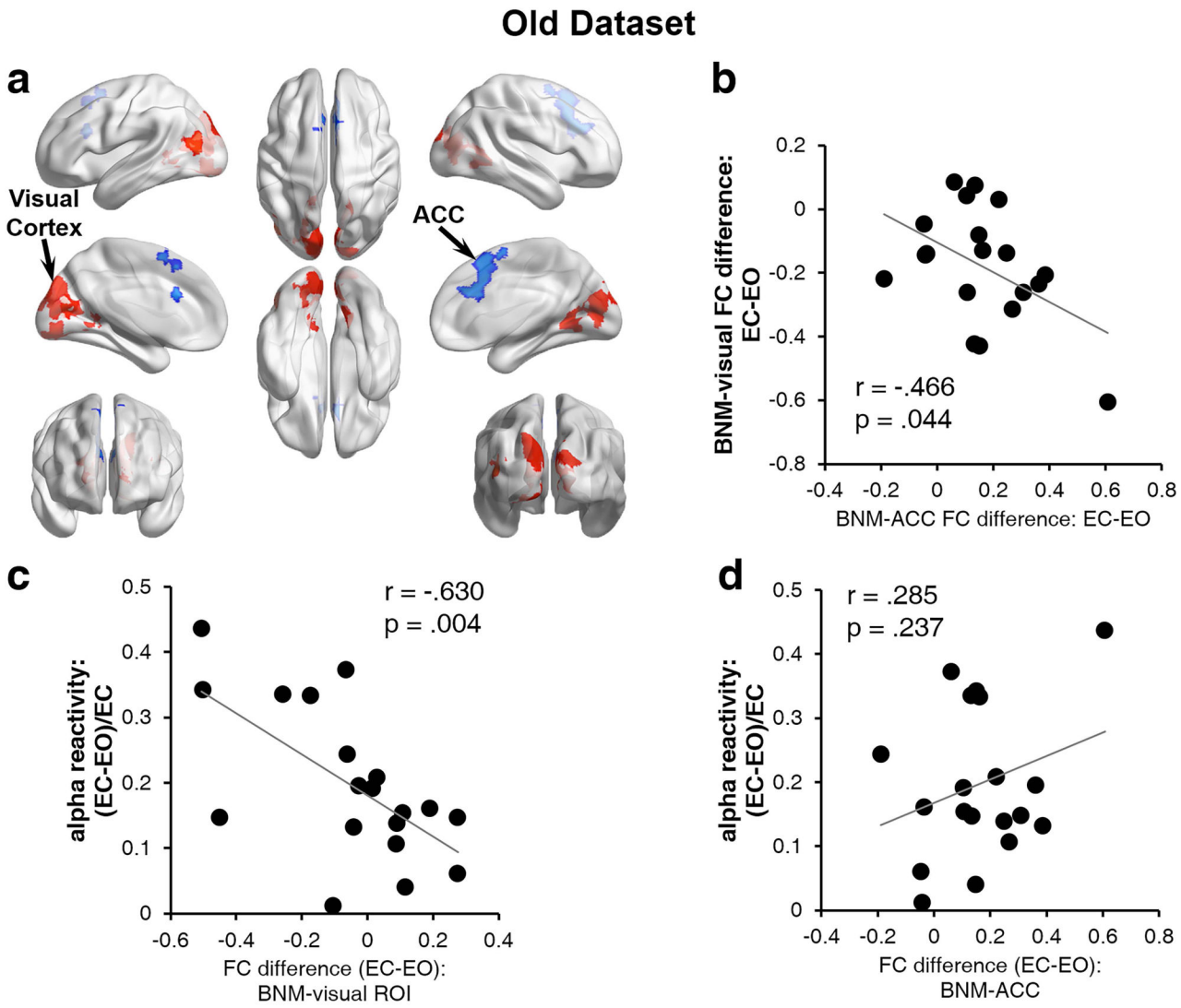

FIGURE 4. BNM-seeded functional connectivity and alpha reactivity for older adults.

(a) Brain areas showing increased (warm color) and decreased (cool color) functional connectivity to BNM from the EC to EO ($p<0.05$, corrected for multiple comparisons via FDR). (b) The EC-to-EO difference of BNM-ACC functional connectivity negatively correlated with that of BNM-visual functional connectivity. (c) Alpha reactivity was negatively correlated with the EC-to-EO difference in BNM-visual functional connectivity. (d) Alpha reactivity was not correlated with the EC-to-EO difference in BNM-ACC functional connectivity.

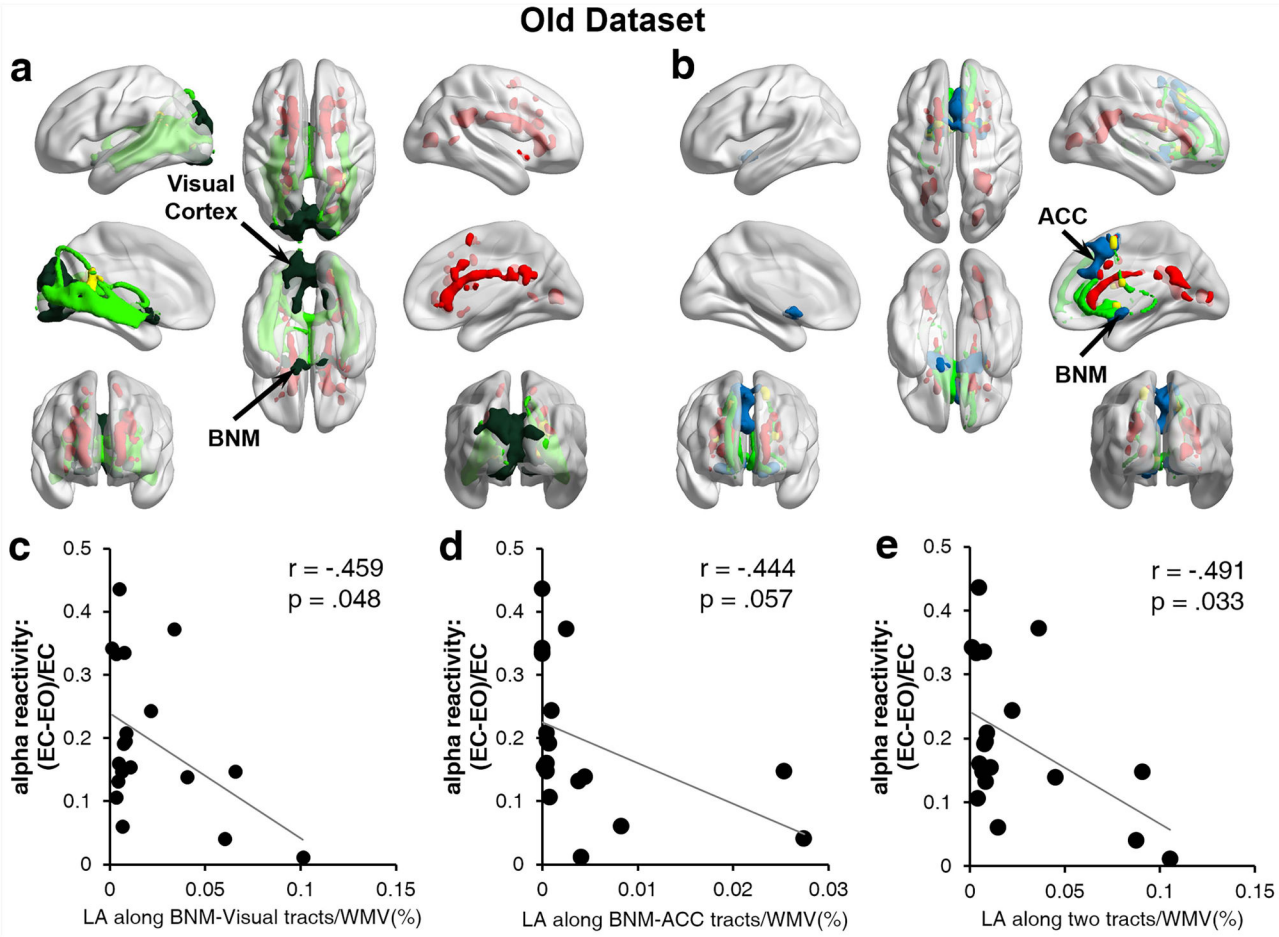

FIGURE 5. LA and alpha reactivity for old adults.

(a) LA distribution (Red) along the fiber tracts from BNM (dark green) to visual cortex (dark green) for a sample subject. Red: LA distribution in the whole brain. Light green: fiber tracts from BNM to visual cortex. (b) LA distribution (red) along the fiber tracts from BNM (blue) to ACC (blue) for a sample subject. Red: LA distribution in the whole brain. Light green: fiber tracts from BNM to ACC. (c) Alpha reactivity was negatively correlated with LA volume along BNM-visual fiber tracts. (d) Alpha reactivity was moderately correlated with LA volume along BNM-ACC fiber tracts. (e) Sum of LA volume along BNM-visual and BNM-ACC fiber tracts was negatively correlated with alpha reactivity. WMV: white matter volume. ACC: anterior cingulate cortex.

Table I.

Demographic information of older participants (N=40)

Variable	Mean	SD	Minimum	Maximum
Age (years)	70.18	6.73	60.00	85.00
Male: Female	22:18			
Education (years)	16.66	2.45	12.00	24.00
TICS *	38.73	2.93	32.00	45.00

* TICS=Telephone Interview for Cognitive Status

Table II.

Subset of older participants who completed EC and EO EEG recordings (N=19)

Variable	Mean	SD	Minimum	Maximum
Age (years)	71.47	7.55	60.00	85.00
Male: Female	13:6			
Education (years)	17.16	2.69	13.00	24.00
TICS	38.21	2.96	32.00	44.00
LA, raw (mm^3)	7786.26	10436.13	562.00	45421.00
White Matter, raw (mm^3)	439870.24	49940.82	355277.63	560833.03
%White Matter	0.02	0.02	0.00	0.10